FEM ANALYSIS OF RADIAL-AXIAL PROFILE RING ROLLING PROCESS

Zhengkun Feng[(a)], Henri Champliaud[(b)]

Department of Mechanical Engineering,
Ecole de technologie superieure
1100 Notre-Dame Street West,
Montreal, Quebec, H3C 1K3, Canada

[(a)]zhengkun.fengca@etsmtl.ca, [(b)]henri.champliaud@etsmtl.ca

ABSTRACT
Profile radial-axial ring rolling is widely used for producing critical structural components in many industries. This complex bulk forming process is characterized by high nonlinearity, unsteady three-dimensional deformation and dynamic contact boundary conditions caused by the rotations of ring and rolls. In this paper, a numerical model based on finite element approach with non-uniform mesh of mixed cubic and tetrahedral elements is proposed to simulate and analyze the process. A large expanded ring with T-profile section has been obtained by numerical simulations.
Keywords: Profile radial-axial ring rolling, Finite element analysis, Residual stress, Bulk forming

1. INTRODUCTION
Ring rolling is widely used to produce seamless rings for critical structural components due to the advantages over the alternative processes (Allwood, Tekkaya, and Stanistreet 2005a). However, the trial and error technique still used in manufacture is intensive energy, time and labor consuming. As the fast evolution in computing technology has significantly reduced CPU time, more accurate analyses of the process can be performed by modeling and simulations.

Radial-axial ring rolling is characterized by unsteady three-dimensional deformation and high nonlinearity that have significant effects on the deformation behaviors of the process, as well as the mechanical properties and microstructure of the expanded rings. Although ring rolling process exists in manufacture more than one hundred years (Eruç and Shivpuri 1992a and 1992b), the process was mainly studied with experimental and theoretical methods prior to the 1990's (Johnson and Needham 1968). However, the process modeling based on finite element method becomes increasingly an important research subject due to the evolution of computing capacity. Utsunomiya et al. (2002) analyzed a cold ring rolling process with a two-dimensional finite element model because three-dimensional models required large computational time. Song et al. (2002) established also a two-dimensional model to simulate hot ring rolling process. Joun et al. (1998) established a viscoplastic model to investigate the process. Moon et al. (2008) analyzed the origin of the polygonal-shaped defects in hot ring rolling process. Casotto et al. (2005) evaluated the sensitivity of cooling parameters to the ring defects of hot ring rolling process and the geometry of hot rolled rings at room temperature after cooling with a two-dimensional finite element model. Hua et al. (2009) established a finite element model to investigate the behaviors of cold ring rolling process. Yea et al. (2003) investigated the roll force, pressure distribution and contact length using a three-dimensional finite element model. The unsteady three-dimensional behaviors, high nonlinearity and the dynamic contact boundary caused by the continuous rotations of the ring and rolls consume large computing time. In order to reduce CPU consuming, Davey and Ward (2003) used the ALE formulation, and Ranatunga et al. (2004) used the Upper Bound Elemental technique. Forouzan et al. (2003a and 2003b) used a thermal spoke method to simulate the idle roll without considering the nonlinearity to reduce computational time. The explicit finite element model has been used by many investigators, including Wang et al. (2006), to increase computational efficiency.

Profile radial-axial ring rolling is more complex, particularly due to the geometry of the sections. A number of attempts have been made to study this process. In the 1970's, Mamalis et al. (1976) investigated experimentally the process. They analyzed the effects of mandrel feed rate, the initial section and the thickness reduction of the ring on the metal spread and the flow patterns. Recently, researches on hot radial-axial ring rolling process for large and profile rings and analyses of the microstructure, strain and stress distributions of rolled rings have increased: Yeom et al. (2007) investigated an optimum hot ring rolling process for a large-scale ring of Ti–6Al–4V alloy using FE analysis; Hua et al. (2007) established an analytical model for the motion of a guide roll in a profile ring rolling process; Kim et al. (2007) developed a profile ring rolling process to simulate the strain distributions in the deformation zone of large slewing rings; Hua et al. (2009) determined the relationship between deformation behaviors and the feed amount during cold ring rolling process for a small ring with L profile section; Allwood et al. (2005b) evaluated the influence of process asymmetry on the stability of incremental ring rolling; Ryttbery et al. (2010) investigated the relationship between the deformation and the evolution of the microstructure and the texture of the ring in a cold ring rolling process; The influence of the ratio of feed rate per revolution at the main roll side to that at the idle roll side on the evolution of stress and strain was investigated by Wang (2011). However, publications are still rare on the subject of comprehensive analyses for hot radial-axial ring rolling process with large diameters and with profile sections.

Since the process is complex and characterized by highly nonlinear behaviors, unsteady three-dimensional deformation, continuous local forming, this research is focusing on establishment of a comprehensive model to predict the applied forces and the effects of process parameters on the shape of the expanded rings. The objective of this research is to obtain seamless rolled rings with uniform quality, smooth surface, short production time and less material loss. Investigation of the process behaviors will be carried out to analyze the geometry defects that relate to process parameters, the stress and strain, and the residual stress analyses. This paper provides preliminary investigation of radial-axial ring rolling process with profile sections based on finite element analysis with non-uniform mesh of mixed cubic and tetrahedral elements. Firstly, a numerical model based on finite element approach using the well-known ANSYS/LS-DYNA software for the process is built. Then, the simulation results are represented and discussed.

2. GEOMETRICAL SET UP AND OPERATING SEQUENCE

A profile radial-axial ring rolling machine may consist of a main roll, a mandrel, two conical rolls, and a doughnut-shaped blank used as initial ring (Fig. 1). There is a circumferential groove in the mid height of the mandrel to make a profile surface for the internal surface of the ring as illustrated on the top right corner of this figure. The conical rolls, with contacts on the upper and lower surfaces of the ring, locate at the opposite position to the contact surfaces of the radial rolls. The main roll is a driving roll which rotates around its stationary axis at a constant angular velocity, and drives the ring to rotate by the friction on their contact surfaces. The mandrel is an idle roll which advances at a constant feed rate towards the main roll. The radial pass between the main roll and the mandrel reduces the ring thickness by compression in the radial direction. Consequently, the ring diameter expands. Meanwhile, the two conical axial rolls rotate in opposite directions around their stationary axes and press towards each other for the purpose of creating an axial compression pass to reduce the ring height. In addition, they provide the stability and prevent from fishtail defects on the upper and lower surfaces of the expanded rings.

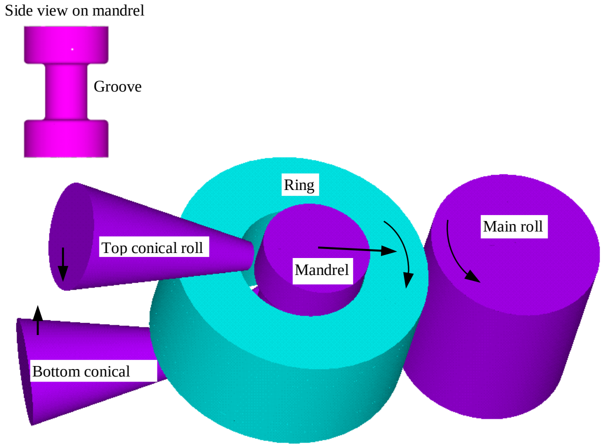

Figure 1: Geometrical set up

3. PROCESS MODELING BASED ON FINITE ELEMENT METHOD

The dynamic explicit three-dimensional model for simulating the profile radial-axial ring rolling process was illustrated in Figure 2. The numerical model was created on ANSYS/LS-DYNA platform. The height, the internal and external radii of the ring were 1.0 m, 0.5 m and 1.0 m, respectively. The radii of the main roll and the mandrel were 0.665 m and 0.42 m, respectively and their heights were 1.4 m. The groove width and depth were 0.6 m and 0.5 m, respectively. The groove was axisymmetrical to the mandrel axis and symmetrical to the plane perpendicular to this axis which located at the mid height of the mandrel. Each conical roll had top radius of 0.112 m, bottom radius of 0.42 m and height of 1.5 m. The ring, the mandrel and the main roll were meshed with 8-node cubic elements. The mesh in the contact zones with the corners of the mandrel was refined and meshed with linear 4-node tetrahedral elements (Fig. 2b) because the larger deformation of the ring occurred at these locations (See the following section of Simulation results and discussions). The tetrahedral elements were derived from cubic elements. Each cubic element to be derived was divided into six tetrahedral elements without additional nodes. The six vertexes of each cubic element to be derived were the vertexes of the six tetrahedral elements. In addition, Flanagan-Belytschko stiffness form with exact volume integration for cubic elements was used for hourglass control (Flanagan and Belytschko 1981). The model was assumed as isotherm and the mechanical properties at temperature of 800 °C were used. Elastic perfectly plastic property was used for the material model of the ring. The elastic modulus, yield stress, Poisson's ratio and density of the ring were 92 GPa, 134 MPa, 0.3 and 7850 kg/m^3, respectively. The mandrel and the main roll were meshed with the same element type as the ring. There was only one cubic element through the thickness for the mandrel. For the ring, there were 79360 elements of which 61440 elements were tetrahedral elements. There were 32384 nodes in total and 10 cubic elements through the thickness. The mandrel was assumed as elasto-plastic with very high yield stress (1800 GPa) to provide better contacts with the ring surfaces during the process. The conical rolls and the main roll were assumed as rigid bodies and the conical rolls were meshed with 4-node shell elements. There was only one 5-integration-point element through thickness for the conical rolls and one cubic element through the thickness for the main roll. The static and dynamic friction coefficients on the contact surface of ring with main roll and with mandrel were assumed constant as 0.6. No friction was assumed on the contact surfaces of ring with the conical rolls so that the conical rolls had no rotation. Automatic surface-to-surface contact type was selected for these contact surfaces. The speed of the main roll and the feed rate of the mandrel were assumed as constants.

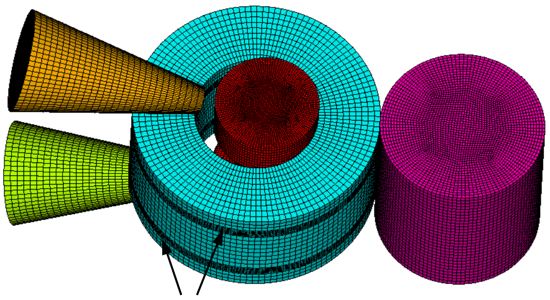

(a) FEM model

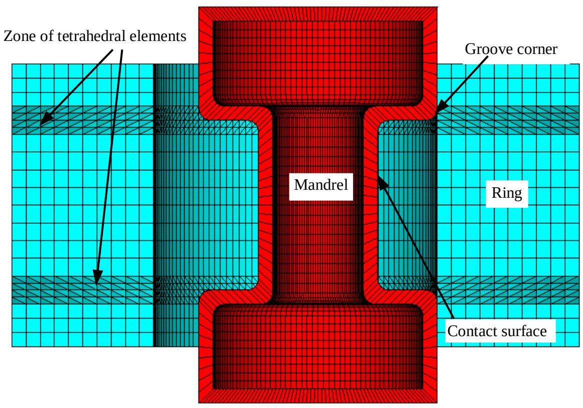

(b) Sectional view on contact surface between the ring and the mandrel

Figure 2: Three-dimensional profile radial-axial ring rolling model

4. SIMULATION RESULTS AND DISCUSSIONS

The total simulation time was 1000 seconds in the numerical simulation with the model described in the previous section. The time step was selected as 10^{-4} seconds. The speed of the main roll and the feed rate of the mandrel were 0.17 rad/s and 0.75 mm/s, respectively. For simplicity, a small feed rate was applied to the conical rolls during the simulation to keep the stability of the system. At the end of the simulation, an expanded profile ring on the right side in Fig. 3a was obtained from the initial ring with rectangular profile shown on the left side. Figure 3b shows the expanded profile ring with internal radii R_1 and R_2 of 0.725 m, 1.17 m and external radius R_3 of 1.37 m as shown on the cutting section A-A in Fig. 3a. Figure 4 shows the Von Mises strain distribution on a top view of the expanded ring surface. The maximal strains were located in the narrower portion of the radial compression pass and near the contact surface with the mandrel. As the ring had clockwise rotation due to the friction on the contact surface with the main roll, the strain on the lower part in the figure was higher than that on the upper part of ring. It was much more significant on the ring internal surface which had the radius of R_2 (See Fig. 3b). It was also observed from the top view in this figure that the strain decreased along the ring rotational direction from exit to entrance due to the progressive compression through the radial compression pass. Figure 5 shows the three principal strain distributions on the cutting section A-A in Fig. 3a. All of the three distributions and the deformed ring shape were symmetrical about the plane perpendicular to ring axis which is located at the mid height of the expanded ring. The first principal strain was the hoop strain which was positive at every point in the section (Fig. 5a). The second principal strain was the axial strain which was negative in the zone near the mid height of the ring and positive near the zones near the ends of the ring (Fig. 5b). The third principal strain was the radial strain which was negative at every point in the section (Fig. 5c). Figure 6 shows another cutting sectional view of the three principal strain distributions of the expanded ring. The cutting section was the symmetrical plane which was the plane perpendicular to ring axis and located at the mid height of the expanded ring. The first principal strain which presented the hoop strain was extension strain everywhere in the section (Fig. 6a). The second principal strain which presented the axial strain was compression strain everywhere in the section (Fig. 6b). The third principal strain which presented the radial strain was also compression strain everywhere in the section (Fig. 6c). As the feed rate of the conical rolls was very small, the axial strain was less than those in the other two directions and it is also observed in Fig. 5.

5. CONCLUSIONS

A numerical model for profile radial-axial ring rolling has been established for analyzing the process behavior. Almost well expanded ring has been obtained by numerical simulations. The non-uniform mesh with linear 8-node cubic elements and 4-node tetrahedral elements has been used. The Flanagan-Belytschko stiffness form with exact volume integration has been used to control hourglass of cubic elements. The results show that the strain distributions on the expanded ring have much different patterns from radial-axial ring rolling for rectangular sections (Feng and Champliaud 2013). The future work will focus on establish a model for expanded ring with more accurate profiles and validate the model with experimental results.

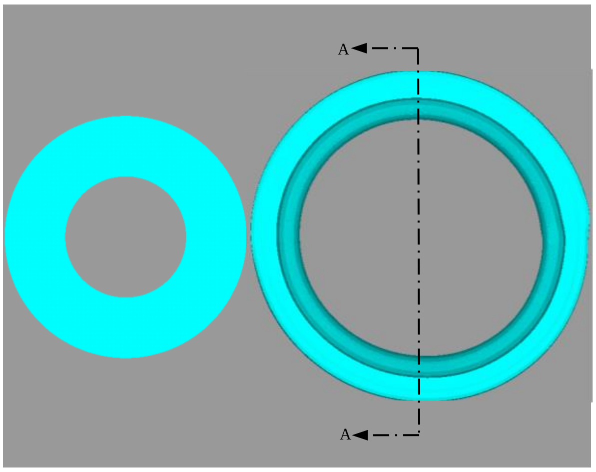

(a) Initial blank (left) and expanded ring (right)

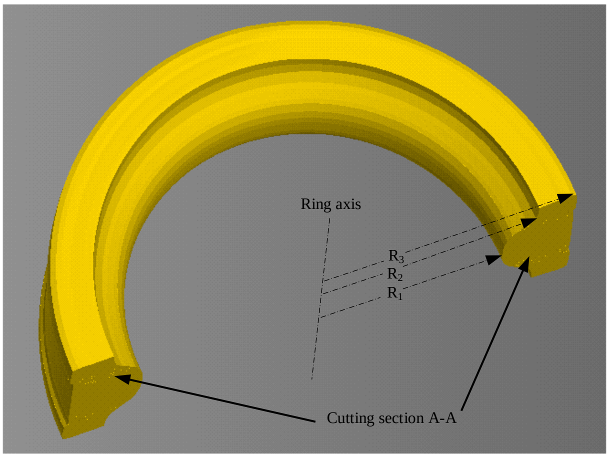

(b) Sectional view on cutting section A-A
Figure 3: Obtained expanded ring

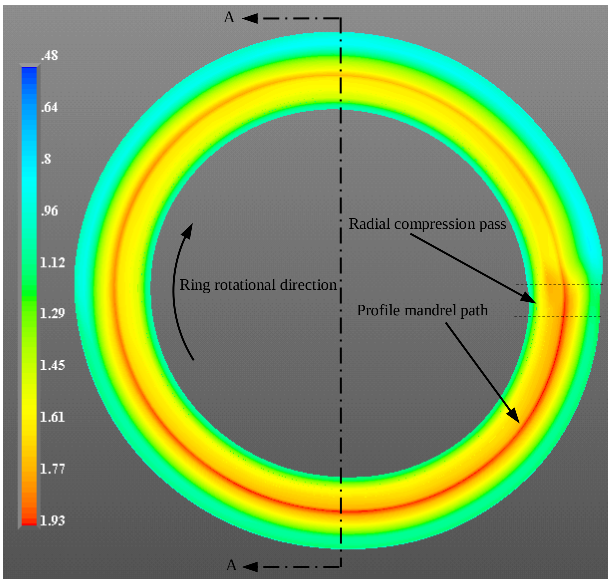

Figure 4: Distribution of Von Mises strain on the top surface of the expanded ring

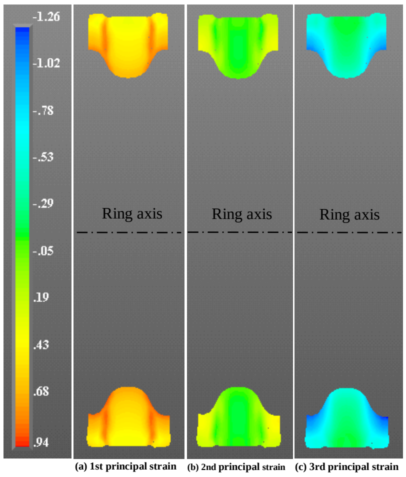

Figure 5: Distributions of the three principal strains on the cutting section A-A of the expanded ring

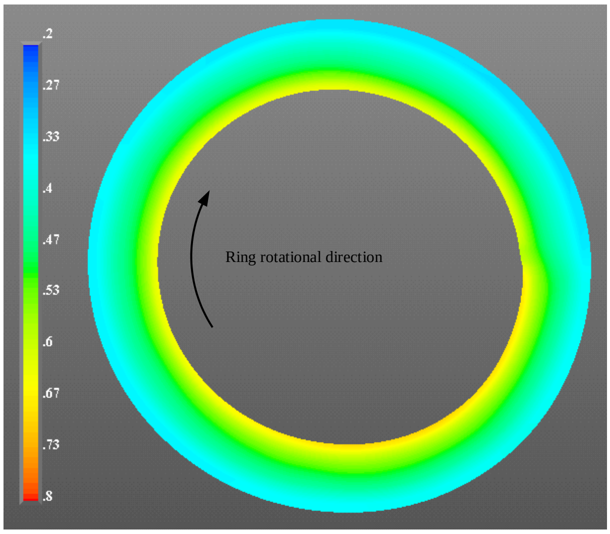

(a) Distribution of the first principal strain

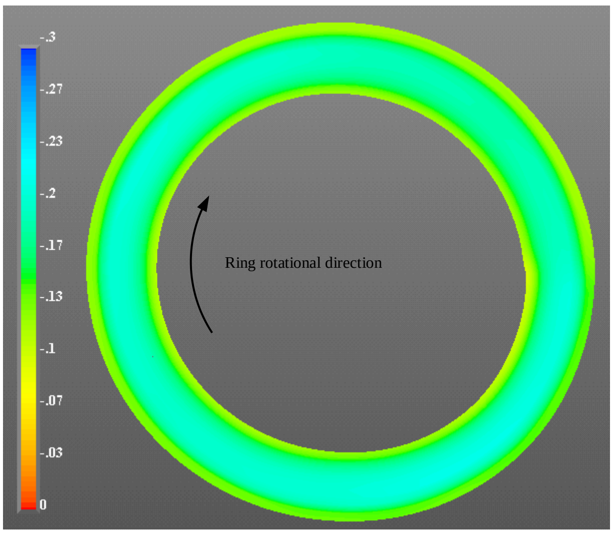

(b) Distribution of the second principal strain

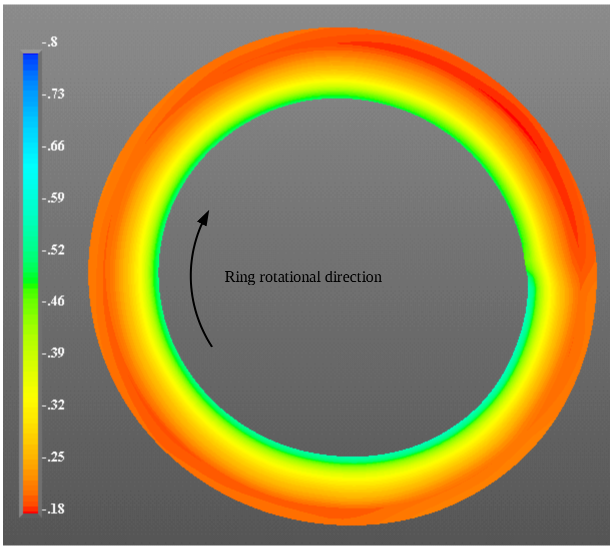

(c) Distribution of the third principal strain

Figure 6: Distributions of the three principal strains on the cutting section A-A of the expanded ring

ACKNOWLEDGMENTS
The authors thank the Natural Sciences and Engineering Research Council (NSERC) for the financial support to this research.

REFERENCES

Allwood, J.M., Tekkaya, A.E. and Stanistreet, T.F., 2005a. The development of ring rolling technology. *Steel Research International*, 76(2-3), 111-120.

Allwood, J.M., Kopp, R., Michels, D., Music, O., Oztop, M., Stanistreet, T.F., Tekkaya, A.E., Tiedemman, I., 2005b. The Technical and Commercial Potential of an Incremental Ring Rolling Process. *CIRP Annals - Manufacturing Technology*, 54(1), 233-236.

Casotto, S., Pascon, F., Habraken, A.M., Bruschi, S., 2005. Thermo-mechanical-metallurgical model to predict geometrical distortions of rings during cooling phase after ring rolling operations. *International Journal of Machine Tools and Manufacture*, 45(6), 657-664.

Davey, K. and Ward, M.J., 2003. An ALE approach for finite element ring-rolling simulation of profiled rings. *Journal of Materials Processing Technology*, 139(1-3), 559-566.

Eruç, E. and Shivpuri, R., 1992a. A summary of ring rolling technology - I. Recent trends in machines, processes and production lines. *International Journal of Machine Tools and Manufacture*, 32(3), 379-398.

Eruç, E. and Shivpuri, R., 1992b. A summary of ring rolling technology - II. Recent trends in process modeling, simulation, planning, and control. *International Journal of Machine Tools and Manufacture*, 32(3), 399-413.

Feng, Z. and Champliaud, H. 2013. Modeling and simulation of hot radial-axial ring rolling process for producing power plant parts. *Materials Science and Technology Conference and Exhibition*, 2013, MS and T 2013, pp. 677-686. October 27-31, Montreal (Quebec, Canada).

Flanagan, D.P. and Belytschko, T., 1981. A Uniform Strain Hexahedron and Quadrilateral With Orthogonal Hourglass Control. *International Journal for Numerical Methods in Engineering*, 17 (5), 679-706.

Forouzan, M.R., Salimi, M., Gadala, M.S., Aljawi, A.A., 2003a. Guide roll simulation in FE analysis of ring rolling. *Journal of Materials Processing Technology*, 142(1), 213-223.

Forouzan, M.R., Salimi, M. and Gadala, M.S., 2003b. Three-dimensional FE analysis of ring rolling by employing thermal spokes method. *International Journal of Mechanical Sciences*, 45(12), 1975-1998.

Hua, L., Qian, D.S. and Pan, L.B., 2009. Deformation behaviors and conditions in L-section profile cold ring rolling. *Journal of Materials Processing Technology*, 209(11), 5087-5096.

Hua, L., Zuo, Z.J., Lan, J. and Qian, D.S., 2007. Research on following motion rule of guide roller in cold rolling groove ball ring. *Journal of Materials Processing Technology*, 187-188(0), 743-746.

Johnson, W. and Needham, G., 1968. Experiments on ring rolling. *International Journal of Mechanical Sciences*, 10(2), 95-113.

Joun, M.S., Chung, J.H. and Shivpuri, R., 1998. An axisymmetric forging approach to preform design in ring rolling using a rigid–viscoplastic finite element method. *International Journal of Machine Tools and Manufacture*, 38(10–11), 1183-1191.

Kim, K.H., Suk, H.G. and Huh, M.Y., 2007. Development of the profile ring rolling process for large slewing rings of alloy steels. Journal of Materials Processing Technology, 187-188(0), 730-733.

Mamalis, A.G., Hawkyard, J.B. and Johnson, W., 1976. Spread and flow patterns in ring rolling. International Journal of Mechanical Sciences, 18(1), 11-16.

Moon, H.K., Lee, M.C. and Joun, M.S., 2008. Predicting polygonal-shaped defects during hot ring rolling using a rigid-viscoplastic finite element method. *International Journal of Mechanical Sciences*, 50(2), 306-314.

Ranatunga, V., Gunasekera, J.S., Vaze, S.P., De Souza, U., 2004. Three-Dimensional UBET Simulation Tool for Seamless Ring Rolling of Complex Profiles. *Journal of Manufacturing Processes*, 6(2), 179-186.

Ryttberg, K., Knutson Wedel, M., Recina, V., Dahlman, P., Nyborg, L., 2010. The effect of cold ring rolling on the evolution of microstructure and texture in 100Cr6 steel. *Materials Science and Engineering: A*, 527(9), 2431-2436.

Song, J.L., Dowson, A.L., Jacobs, M.H., Brooks, J., Beden, I., 2002. Coupled thermo-mechanical finite-element modelling of hot ring rolling process. *Journal of Materials Processing Technology*, 121(2-3), 332-340.

Utsunomiya, H., Saito, Y., Shinoda, T, Takasu, I., 2002. Elastic-plastic finite element analysis of cold ring rolling process. *Journal of Materials Processing Technology*, 125-126(0), 613-618.

Wang, M., Yang, H., Sun, Z., Guo, L., Ou, X., 2006. Dynamic explicit FE modeling of hot ring rolling process. *Transactions of Nonferrous Metals Society of China*, 16(6) 1274-1280.

Wang, M., 2011. Comparison of evolution laws of stress and strain fields in hot rolling of titanium alloy large rings with different sizes. *Transactions of Nonferrous Metals Society of China*, 21(7), 1611-1619.

Yea, Y., Ko, Y., Kim, N., Lee, J., 2003. Prediction of spread, pressure distribution and roll force in ring rolling process using rigid-plastic finite element method. *Journal of Materials Processing Technology*, 140(1-3), 478-486.

Yeom, J.T., Kim, J.H., Park, N.K., Choi, S.S., Lee, C.S., 2007. Ring-rolling design for a large-scale ring product of Ti-6Al-4V alloy. *Journal of Materials Processing Technology*, 187-188(0), 747-751.